The Astronomical Journal, 124:1064–1076, 2002 August

CHROMOSPHERICALLY ACTIVE STARS. XXI. THE GIANT, SINGLE-LINED BINARIES HD 89546 AND HD 113816

Francis C. Fekel,[1] Gregory W. Henry, and Joel A. Eaton
Center of Excellence in Information Systems, Tennessee State University, 330 10th Avenue North, Nashville, TN 37203;
fekel@evans.tsuniv.edu, henry@schwab.tsuniv.edu, eaton@donne.tsuniv.edu

Julius Sperauskas
Vilnius University Observatory, Ciurlionio 29, Vilnius 2009, Lithuania; julius.sperauskas@ff.vu.lt

and

Douglas S. Hall
Dyer Observatory, Vanderbilt University, Nashville, TN 37235; hall@astro.dyer.vanderbilt.edu
Received 2002 March 11; accepted 2002 May 2

ABSTRACT

We have obtained spectroscopy and photometry of the chromospherically active, single-lined spectroscopic binaries HD 89546 and HD 113816. HD 89546 has a circular orbit with a period of 21.3596 days. Its primary has a spectral type of G9 III and is somewhat metal-poor with [Fe/H] ~ -0.5. HD 113816 has an orbit with a period of 23.6546 and a low eccentricity of 0.022. Its mass function is extremely small, 0.0007 $M_{\odot}$, consistent with a very low inclination. The primary is a slightly metal-poor K2 III. A decade or more of photometric monitoring with an automatic telescope demonstrates that both systems display brightness variations due to rotational modulation of the visibility of photospheric star spots, as well as light-curve changes resulting from the redistribution of star spots by differential rotation and long-term changes in the filling factor of the spots. We determined rotation periods for each season when the observations were numerous enough. Our mean rotation periods of 21.3 and 24.1 days for HD 89546 and HD 113816, respectively, confirm that the giants in each system are synchronously rotating. The orbital elements and properties of the giant components of these two systems, including levels of surface magnetic activity, are quite similar. However, the two rotational inclinations are rather different, 57° for HD 89546 and 13° for HD 113816. Thus the latter giant is seen nearly pole on. We analyzed the light curves for similarities and differences that result from viewing these two systems from quite different inclinations.

Key words: binaries: spectroscopic — stars: spots — stars: variables: other
On-line material: machine-readable tables

1. INTRODUCTION

Chromospherically active stars have been identified in spectroscopic surveys by their strong Ca II H and K emission. In particular, such active stars have been found in objective-prism surveys (e.g., Bidelman & MacConnell 1973; Bidelman 1981) and more recently in the moderate- and high-resolution spectroscopic searches of Henry et al. (1996) and Strassmeier et al. (2000), respectively. Over the past several decades X-ray and ultraviolet surveys with satellites have proved to be another very effective way of finding active, late-type stars. The observations produced by satellites such as *HEAO 1*, *Einstein*, *EXOSAT*, *EUVE*, and *ROSAT* have led to optical identifications (e.g., Buckley et al. 1987; Fleming, Gioia, & Maccacaro 1989; Cutispoto et al. 1991; Tagliaferri et al. 1994; Jeffries, Bertram, & Spurgeon 1995; Neuhaüser et al. 1997; Cutispoto et al. 1999) of many chromospherically active stars. Here we discuss two such stars, one discovered from an objective-prism survey and the second found as a result of *HEAO 1* observations.

HD 89546 = FG Ursae Majoris ($\alpha = 10^{h}21^{m}47\overset{s}{.}5$, $\delta = 60°54'46''$ [J2000.0], $V = 7.26$ mag) was initially identified as a chromospherically active star from an examination of objective-prism plates by W. Bidelman (1991, private communication). As a result, follow-up photometry and spectroscopy were obtained.

Strassmeier (1994) and Strassmeier et al. (1994) confirmed that HD 89546 has quite strong Ca II H and K emission. Other indications of chromospheric and coronal activity also have been detected. Henry, Fekel, & Hall (1995) found that the Hα absorption line is significantly filled with emission, and in one spectrum a blueshifted emission feature rose above the continuum (see Fig. B2 in Strassmeier et al. 2000 for a similar spectrum). Figure 13 of Montes et al. (2000) shows additional indications of strong activity. Two of the Ca II IR triplet lines and even the Hβ absorption line are partially filled with emission. In their *ROSAT* catalog of high-latitude sources Schwope et al. (2000) gave HD 89546 as the optical counterpart to a weak X-ray source.

From four seasons of photometry Henry et al. (1995) detected light variability with a period of 21.5 days plus variability on a significantly longer timescale. The discovery of light variations led Kazarovets & Samus (1997) to assign HD 89546 the variable star name FG UMa. Henry et al. (1995) reported that Dadonas found HD 89546 to be a sin-

[1] Visiting Astronomer, Kitt Peak National Observatory, National Optical Astronomy Observatory, which is operated by the Association of Universities for Research in Astronomy, Inc. under cooperative agreement with the National Science Foundation.

gle-lined binary with a circular orbit and a period of 21.3 days, making the primary a synchronously rotating star. Recently, Marino et al. (2002) published a radial-velocity curve and a complete set of orbital elements for HD 89546.

From several red-wavelength spectra, Henry et al. (1995) determined a spectral type of G8 IV, although other data suggested that a luminosity class of III–IV might be more appropriate. Marino et al. (2002) found that a rotationally broadened spectrum of HR 3422, a K0 III, reproduced their high-resolution echelle spectra of HD 89546. Active late-type stars are expected to be rapidly rotating, and HD 89546 is no exception. Fekel (1997) revised the $v \sin i$ value of the primary from 15 km s^{-1} (Henry et al. 1995) to 18 km s^{-1}.

HD 113816 = IS Virginis ($\alpha = 13^{h}06^{m}26\overset{s}{.}0$, $\delta = -04^{\circ}50'45''$ [J2000.0], $V = 8.27$ mag) first came to prominence with its identification as the optical counterpart to an X-ray source observed by the *HEAO 1* satellite (Buckley et al. 1987). From 15 blue-wavelength spectroscopic observations Buckley et al. (1987) found the star to have strong Ca II H and K emission and relatively low-amplitude radial velocity variations. They concluded that HD 113816 likely has a period greater than 20 days and possibly a low orbital inclination. They estimated a spectral classification of K2 IV–III from its photometric colors and a projected rotational velocity of 30 ± 10 km s^{-1}.

The discovery that HD 113816 is a chromospherically active star prompted its inclusion in various surveys. Randich, Giampapa, & Pallavicini (1994) observed the system as part of a lithium survey of RS CVn binaries. They found a log lithium abundance of 0.8 and an iron abundance [Fe/H] = −0.9. They obtained a significantly lower $v \sin i$ of 10 km s^{-1}, while Fekel (1997) determined an even smaller value of 5.9 km s^{-1}. Strassmeier (1994) showed that, in addition to the extremely strong Ca II H and K emission, the Balmer Hϵ line of HD 113816 is in emission. Dempsey et al. (1993) detected the soft X-ray flux of HD 113816 from observations with *ROSAT*. Henry et al. (1995) determined a spectral type of K0 III and estimated an orbital inclination of 11°. They reported that Dadonas found HD 113816 to be a binary with an orbital period of 23.7 days, a semiamplitude of 6.7 km s^{-1}, and an essentially circular orbit. Henry et al. (1995) obtained six seasons of photometric data. The star showed both long-term and short-term light variability, with the latter having a period of 23.5 days. Adopting this value as the rotation period, they concluded that the K giant is synchronously rotating. Strassmeier et al. (1997) confirmed the light variability period, computing a mean value of 23.67 days from four additional seasons of photometry. As a result of the detection of such light variations, Kazarovets & Samus (1997) gave HD 113816 the variable star name IS Vir.

2. SPECTROSCOPIC OBSERVATIONS AND REDUCTIONS

From 1991 June to 1999 May we collected 27 high-resolution spectrograms of HD 89546. Observations were made with the Kitt Peak National Observatory (KPNO) coudé feed telescope, coudé spectrograph, and a TI CCD detector. Most of the KPNO spectrograms are centered in the red at 6430 Å, cover a wavelength range of about 80 Å, and have a resolution of 0.21 Å. In addition, two observations were obtained of the Hα region and two of the lithium region. The spectra have typical signal-to-noise ratios of 150–200.

A second set of 27 velocities was obtained with Coravel-type spectrometers used at three observatories. The characteristics of those spectrometers have been discussed by Tokovinin (1987) and Upgren, Sperauskas, & Boyle (2002). In 1993 February and March observations were obtained with the 1 m telescope at Mount Maidanak, Uzbekistan. In 1999 March and April additional observations were collected with the 1.65 m telescope at Moletai Observatory in Lithuania. Finally, in 2000 March two observations were made with the 1.54 m telescope of Steward Observatory on Mount Bigelow. All of these radial velocities for HD 89546 are listed in Table 1, along with their corresponding orbital phases and velocity residuals computed from the orbit determined in § 4.1.

From 1992 May to 2000 April we obtained 37 high-resolution spectrograms of HD 113816 with the previously mentioned KPNO telescope, spectrograph, and detector system. All KPNO spectrograms are centered in the red at 6430 Å, and they have the same wavelength range and resolution as those of HD 89546. The spectra have typical signal-to-noise ratios of 150.

A second set of 31 velocities was obtained with the same Coravel–type spectrometers and telescopes given above for HD 89546. Radial velocities for all of these observations are given in Table 2, along with their corresponding orbital phases and velocity residuals computed from the orbit determined in § 5.1.

We measured the radial velocities of the KPNO spectra with the IRAF cross-correlation program FXCOR (Fitzpatrick 1993). We used the IAU radial-velocity standards HR 4695, β Vir, and 10 Tau as cross-correlation reference stars. Their velocities of 36.5, 4.4, and 27.9 km s^{-1}, respectively, were adopted from Scarfe, Batten, & Fletcher (1990). Radial-velocity reductions with the Coravel spectrometers are briefly discussed in Upgren et al. (2002).

3. PHOTOMETRIC OBSERVATIONS AND REDUCTIONS

Our photometric observations were all obtained with the T3 0.4 m automatic photoelectric telescope (APT) at Fairborn Observatory in the Patagonia Mountains of southern Arizona. The 0.4 m APT uses a temperature-stabilized EMI 9924B photomultiplier tube to acquire data successively through Johnson B and V filters. Each program star was measured each clear night in the following sequence, termed a group observation: *K, S, C, V, C, V, C, V, C, S, K*, in which K is a check star, C is the comparison star, V is the program star, and S is a sky reading. Three $V-C$ and two $K-C$ differential magnitudes are formed from each sequence and averaged together to create group means. Group mean differential magnitudes with internal standard deviations greater than 0.01 mag were rejected to filter the observations taken under nonphotometric conditions. The surviving group means were corrected for differential extinction with nightly extinction coefficients, transformed to the Johnson system with yearly mean transformation coefficients, and treated as single observations thereafter. The external precision of these group means, based on standard deviations for pairs of constant stars, is typically ∼0.004–0.005 mag on good nights with this telescope. Further infor-

TABLE 1

RADIAL VELOCITIES OF HD 89546

HJD −2,400,000	Phase	Velocity (km s^{-1})	$O-C$ (km s^{-1})	Weight	Source[a]
48,427.636	0.266	25.8[b]	−0.8	1.00	KPNO
48,429.659	0.360	13.4	−0.4	1.00	KPNO
48,605.059	0.572	7.7[c]	0.0	1.00	KPNO
48,608.066	0.713	23.4[c]	−0.1	1.00	KPNO
48,769.703	0.280	24.7	0.3	1.00	KPNO
48,774.707	0.515	5.6	0.2	1.00	KPNO
48,913.039	0.991	52.7	0.3	1.00	KPNO
49,101.734	0.825	39.6	0.0	1.00	KPNO
49,104.812	0.969	52.0	0.0	1.00	KPNO
49,302.048	0.203	35.3	−0.4	1.00	KPNO
49,307.982	0.481	4.9	−0.6	1.00	KPNO
49,038.335	0.857	42.0	−1.6	0.15	MMU
49,039.279	0.901	46.9	−1.2	0.15	MMU
49,042.395	0.047	50.8	−0.6	0.15	MMU
49,044.385	0.140	45.9	2.0	0.15	MMU
49,050.307	0.418	11.1	2.7	0.15	MMU
49,052.312	0.511	6.7	1.3	0.15	MMU
49,055.372	0.655	15.6	0.0	0.15	MMU
49,058.336	0.794	32.6	−2.6	0.15	MMU
49,061.363	0.935	49.4	−1.1	0.15	MMU
49,062.315	0.980	53.7	1.4	0.15	MMU
49,063.365	0.029	51.9	−0.2	0.15	MMU
49,064.334	0.074	47.7	−2.2	0.15	MMU
49,065.328	0.121	45.9	−0.1	0.15	MMU
49,461.860	0.685	19.1	−0.5	1.00	KPNO
49,833.769	0.097	47.9	−0.3	1.00	KPNO
49,834.806	0.146	43.2	0.0	1.00	KPNO
49,835.653	0.185	38.0	−0.2	1.00	KPNO
49,836.825	0.240	30.4	0.1	1.00	KPNO
49,838.791	0.332	17.6	0.4	1.00	KPNO
50,199.774	0.233	32.2	0.8	1.00	KPNO
50,203.705	0.417	8.4	−0.1	1.00	KPNO
50,405.032	0.842	42.4	0.6	1.00	KPNO
50,576.656	0.877	46.4	0.6	1.00	KPNO
50,580.634	0.064	51.2	0.6	1.00	KPNO
50,630.639	0.405	9.1	−0.3	1.00	KPNO
50,829.999	0.738	27.4	0.3	1.00	KPNO
50,830.902	0.780	33.4	0.0	1.00	KPNO
51,094.023	0.099	47.6[b]	−0.4	1.00	KPNO
51,258.430	0.796	36.3	0.7	0.15	MOL
51,259.430	0.843	41.7	−0.2	0.15	MOL
51,260.482	0.892	45.9	−1.3	0.15	MOL
51,264.481	0.080	47.6	−2.0	0.15	MOL
51,264.485	0.080	47.6	−1.9	0.15	MOL
51,267.419	0.217	32.8	−0.9	0.15	MOL
51,268.446	0.265	26.4	−0.2	0.15	MOL
51,269.401	0.310	20.1	−0.1	0.15	MOL
51,270.369	0.355	14.8	0.4	0.15	MOL
51,271.353	0.401	11.3	1.6	0.15	MOL
51,304.341	0.946	51.4	0.3	0.15	MOL
51,305.356	0.993	52.0	−0.4	0.15	MOL
51,308.682	0.149	43.1	0.2	1.00	KPNO
51,630.789	0.229	29.9	−2.1	0.15	SO
51,632.691	0.318	21.3	2.2	0.15	SO

[a] MMU = Mount Maidanak, Uzbekistan, KPNO = Kitt Peak National Observatory, MOL = Moletai Observatory, Lithuania, SO = Steward Observatory.

[b] Lithium region, central wavelength 6700 Å.

[c] Hα region, central wavelength 6560 Å.

TABLE 2

RADIAL VELOCITIES OF HD 113816

HJD −2,400,000	Phase	Velocity (km s^{-1})	$O-C$ (km s^{-1})	Weight	Source[a]
48,657.510	0.865	19.5	0.0	0.15	MMU
48,660.317	0.984	24.9	0.4	0.15	MMU
48,660.577	0.995	24.5	−0.4	0.15	MMU
48,663.512	0.119	27.8	0.0	0.15	MMU
48,666.524	0.246	26.8	0.1	0.15	MMU
48,669.459	0.370	23.5	1.0	0.15	MMU
48,672.421	0.495	18.9	1.2	0.15	MMU
48,673.450	0.539	17.7	1.3	0.15	MMU
48,770.719	0.651	14.9	0.2	1.00	KPNO
49,036.509	0.887	21.0	0.6	0.15	MMU
49,038.327	0.964	23.4	−0.3	0.15	MMU
49,038.532	0.973	23.6	−0.4	0.15	MMU
49,042.445	0.138	28.1	0.2	0.15	MMU
49,052.294	0.554	16.9	0.9	0.15	MMU
49,058.280	0.807	17.1	−0.3	0.15	MMU
49,058.530	0.818	16.9	−0.8	0.15	MMU
49,060.516	0.902	21.0	−0.1	0.15	MMU
49,061.396	0.939	23.3	0.6	0.15	MMU
49,062.381	0.981	24.7	0.3	0.15	MMU
49,063.537	0.030	26.3	0.2	0.15	MMU
49,064.413	0.067	27.2	0.2	0.15	MMU
49,065.374	0.107	29.2	1.5	0.15	MMU
49,101.802	0.647	14.9	0.1	1.00	KPNO
49,105.850	0.818	18.3	0.6	1.00	KPNO
49,462.844	0.910	21.4	0.0	1.00	KPNO
49,833.888	0.596	15.3	0.1	1.00	KPNO
49,835.794	0.677	14.4	−0.4	1.00	KPNO
49,837.794	0.761	16.3	0.3	1.00	KPNO
49,838.814	0.805	17.2	−0.1	1.00	KPNO
49,899.735	0.380	22.0	−0.1	1.00	KPNO
49,900.700	0.421	20.4	−0.1	1.00	KPNO
49,901.666	0.462	18.9	0.0	1.00	KPNO
49,902.699	0.505	17.3	−0.1	1.00	KPNO
49,903.752	0.550	15.8	−0.4	1.00	KPNO
50,198.873	0.026	26.1	0.2	1.00	KPNO
50,199.752	0.063	26.8	−0.1	1.00	KPNO
50,200.790	0.107	27.8	0.1	1.00	KPNO
50,201.740	0.147	27.9	0.0	1.00	KPNO
50,202.851	0.194	27.6	0.0	1.00	KPNO
50,203.763	0.233	27.2	0.2	1.00	KPNO
50,265.701	0.851	18.7	−0.3	1.00	KPNO
50,266.654	0.891	20.5	−0.1	1.00	KPNO
50,575.820	0.962	23.5	−0.1	1.00	KPNO
50,576.750	0.001	24.8	−0.3	1.00	KPNO
50,630.690	0.281	25.6	−0.1	1.00	KPNO
50,631.691	0.323	24.3	0.0	1.00	KPNO
50,632.701	0.366	22.7	0.0	1.00	KPNO
50,637.680	0.577	15.9	0.3	1.00	KPNO
50,830.024	0.708	14.6	−0.4	1.00	KPNO
50,830.981	0.748	15.7	0.0	1.00	KPNO
50,832.039	0.793	16.8	−0.1	1.00	KPNO
50,931.774	0.009	25.7	0.3	1.00	KPNO
51,005.681	0.134	27.5	−0.4	1.00	KPNO
51,265.492	0.117	28.1	0.3	0.15	MOL
51,268.518	0.245	27.2	0.5	0.15	MOL
51,302.410	0.678	14.4	−0.4	0.15	MOL
51,303.820	0.738	15.7	0.2	1.00	KPNO
51,304.354	0.760	15.9	−0.1	0.15	MOL
51,304.835	0.781	16.4	−0.1	1.00	KPNO
51,305.370	0.803	17.6	0.4	0.15	MOL
51,306.719	0.860	19.4	0.1	1.00	KPNO
51,307.404	0.889	21.0	0.5	0.15	MOL
51,308.370	0.930	21.9	−0.4	0.15	MOL

TABLE 2—*Continued*

HJD −2,400,000	Phase	Velocity (km s^{-1})	$O-C$ (km s^{-1})	Weight	Source[a]
51,308.740.....	0.946	22.9	0.0	1.00	KPNO
51,311.348.....	0.056	26.7	−0.1	0.15	MOL
51,613.941.....	0.848	19.2	0.4	0.15	SO
51,630.813.....	0.561	14.8	−1.1	0.15	SO
51,657.788.....	0.702	14.9	−0.1	1.00	KPNO

[a] MMU = Mount Maidanak, Uzbekistan, KPNO = Kitt Peak National Observatory, MOL = Moletai Observatory, Lithuania, SO = Steward Observatory.

mation on the operation of the APT can be found in Henry (1995a, 1995b).

The APT acquired 1448 good group means in V and 1460 in B for HD 89546 during 10 observing seasons between 1992 March and 2001 June. The individual $V-C$ and $K-C$ differential magnitudes are given in Table 3.[2] The photometric comparison star was HD 90400 ($V = 6.86$, $B-V = 1.02$, K0), while the check star was HD 91480 = 37 UMa = HR 4141 ($V = 5.16$, $B-V = 0.35$, F1 V).

The APT acquired 910 good group means in V and 946 in B for HD 113816 during 12 observing seasons between 1990 April and 2001 June. Individual $V-K$ and $C-K$ differential magnitudes are given in Table 4 (and see footnote 2). The comparison star for HD 113816 was HD 113449 ($V = 7.69$, $B-V = 0.85$, G5 V), while the check star was HD 111998 = 38 Vir = HR 4891 ($V = 6.11$, $B-V = 0.49$, F5 V). For HD 113816, we created and analyzed the $V-K$ differential magnitudes, rather than the usual $V-C$ differential magnitudes, because the comparison star HD 113449 also turned out to be photometrically variable (see § 5.4).

4. HD 89546 = FG UMa

4.1. *Spectroscopic Orbit*

For HD 89546 a preliminary period of 21.36 days was found from our KPNO radial velocities alone (Table 1). This period was determined by fitting a sine curve to the velocities for trial periods between 1 and 100 days with a step size of 0.01 days. For each period the sum of the residuals squared was computed, and the period with the smallest value of that sum was used as the preliminary value of the orbital period. With this period adopted, initial orbital elements were computed with BISP (Wolfe, Horak, & Storer 1967), a computer program that uses a slightly modified version of the Wilsing-Russell method. This orbit was then refined with SB1 (Barker, Evans, & Laing 1967), a program that uses differential corrections. Similar orbital solutions were determined for the 27 Coravel velocities. The variances of the SB1 solutions for the two sets of velocities resulted in weights of 0.15 for the Coravel velocities relative to the KPNO velocities. A simultaneous solution of the two data sets produced an orbit with a very low eccentricity of 0.0054 ± 0.0062. Thus we computed a circular orbit with SB1C (D. Barlow 1998, private communication), which also uses differential corrections to determine the orbital elements. The tests of Lucy & Sweeney (1971) indicated that the latter solution is to be preferred, and so it is given in Table 5. For a circular orbit the element T, a time of periastron passage, is undefined. Thus, as recommended by Batten, Fletcher, & MacCarthy (1989), T_0, a time of maximum velocity, is listed instead. Orbital phases in Table 1 are computed from these elements. The observed velocities and the computed velocity curve are compared in Figure 1, where zero phase is a time of maximum velocity.

[2] They are also available from the Tennessee State University Automated Astronomy Group Web site at http://schwab.tsuniv.edu/t3/castars21/castars21.html.

TABLE 3

PHOTOMETRIC OBSERVATIONS OF HD 89546

HJD −2,400,000 (1)	$(V-C)_B$ (mag) (2)	$(V-C)_V$ (mag) (3)	$(K-C)_B$ (mag) (4)	$(K-C)_V$ (mag) (5)
48,696.7813.....	0.493	0.519	99.999	−1.709
48,698.7789.....	99.999	0.517	−2.397	−1.712
48,701.7698.....	0.487	0.518	−2.400	−1.712
48,702.7745.....	0.506	99.999	−2.391	−1.720
48,705.7575.....	0.535	0.562	−2.403	−1.700

NOTE.—Table 3 is presented in its entirety in the electronic edition of the Astronomical Journal. A portion is shown here for guidance regarding its form and content.

TABLE 4

PHOTOMETRIC OBSERVATIONS OF HD 113816

HJD −2,400,000 (1)	$(V-K)_B$ (mag) (2)	$(V-K)_V$ (mag) (3)	$(C-K)_B$ (mag) (4)	$(C-K)_V$ (mag) (5)
47,987.8560.....	2.846	2.212	1.961	1.594
47,991.8661.....	99.999	99.999	1.907	1.545
47,993.7065.....	2.846	2.206	1.948	1.616
47,994.8182.....	2.847	2.223	1.960	1.607
47,995.7065.....	2.848	2.222	1.951	1.606

NOTE.—Table 4 is presented in its entirety in the electronic edition of the Astronomical Journal. A portion is shown here for guidance regarding its form and content.

4.2. *Spectral Type*

Strassmeier & Fekel (1990) identified several luminosity-sensitive and temperature-sensitive line ratios in the 6430–6465 Å region. Those critical line ratios and the general appearance of the spectrum were employed as spectral-type criteria. The spectra of HD 89546 were compared with those of late-G and early-K subgiant and giant stars from the lists of Keenan & McNeil (1989) and Fekel (1997), obtained at KPNO with the same telescope, spectrograph, and detector as our spectra of HD 89546. To facilitate a comparison, the spectra of the reference stars were rotationally broadened and shifted in radial velocity with a computer program developed by Huenemoerder & Barden (1984) and Barden (1985). While Henry et al. (1995) previously compared HD 89546 with various subgiants and giants and classified HD 89546 as G8 IV, they noted some discrepancies with both the best spectrum fit and other results. As shown below, the minimum radius of HD 89546 and absolute magnitude from the *Hipparcos* parallax correspond to a luminosity class III star. Thus we compared our spectra of HD 89546 with the spectra of a G8 IV star and several metal-poor giants. The 6430 Å region of HD 89546 is fitted best by spectra of HR

TABLE 5
ORBITAL ELEMENTS OF HD 89546

Parameter	Value
P (days)	21.35957 ± 0.00040
T_0 (HJD)	$2{,}449{,}297.702 \pm 0.020$
γ (km s^{-1})	28.882 ± 0.093
K (km s^{-1})	23.56 ± 0.14
e	0.0 adopted
$a \sin i$ (km)	$6.919 \pm 0.040 \times 10^6$
$f(m)$ ($M_\odot$)	0.02900 ± 0.00051
Standard error of an observation of unit weight (km s^{-1})	0.50

1907 (K0 IIIb, Keenan & McNeil 1989; [Fe/H] = −0.58, Taylor 1999) and HR 4608 (G8 IIIa, Keenan & McNeil 1989; [Fe/H] = −0.46, Taylor 1999). So we classify HD 89546 as a somewhat metal-poor G9 III, having [Fe/H] ∼ −0.5. Our spectral type is in good agreement with the result of Marino et al. (2002), who noted that the spectrum of HR 3422 (K0 III, Upgren & Staron 1970), with lines rotationally broadened to 18 km s^{-1}, produced an excellent match to the spectrum of HD 89546.

4.3. *Basic Properties*

We searched the literature and examined our own data for the brightest known visual magnitude and corresponding $B-V$ of HD 89546. From the APT data in Figure 2 HD 89546 is brightest in season 9, where its differential V magnitude is 0.40. To convert this to an apparent V magnitude, we adopted $V = 6.86$ (ESA 1997) for our comparison star, HD 90400. This resulted in a magnitude at maximum of $V = 7.26$ mag, which is the same as the maximum value given in the recent paper of Marino et al. (2002). O'Neal, Saar, & Neff (1996) showed that on some heavily spotted stars the observed maximum V magnitude underestimates the brightness of the unspotted star by 0.3–0.4 mag. Nevertheless, we have adopted the historical maximum as the unspotted V magnitude of the primary, since for HD 89546 we are unable to determine a specific correction. This magnitude, combined with the *Hipparcos* parallax (ESA 1997) corresponding to a distance of 175 ± 26 pc, resulted in $M_v = 1.05 \pm 0.33$ mag. Since HD 89546 is nearly 50° above the Galactic plane, we assumed no interstellar reddening. A $B-V$ color index of 0.98 mag from our APT data was used in conjunction with Table 3 of Flower (1996) to obtain a bolometric correction and effective temperature. These values were used to compute a luminosity $L = 42.1 \pm 12.8\ L_\odot$ and a radius $R = 9.1 \pm 1.4\ R_\odot$. The uncertainties in the computed quantities are dominated by the uncertainty in

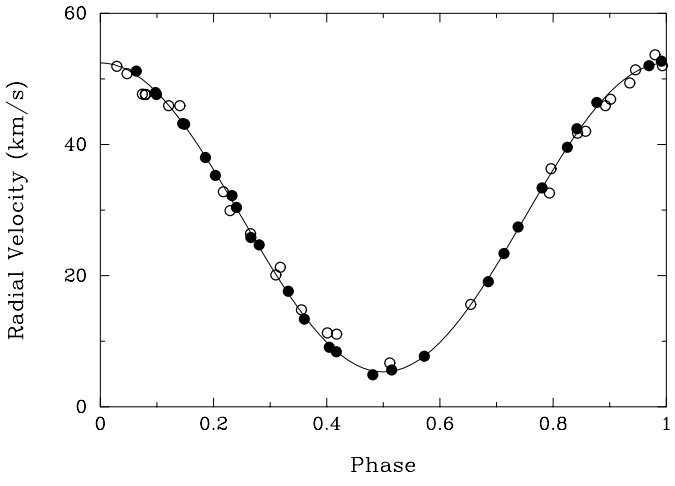

FIG. 1.—Plot of the computed radial-velocity curve of HD 89546 compared with the observations. Filled circles are KPNO velocities; open circles are Coravel velocities. Zero phase is a time of maximum velocity.

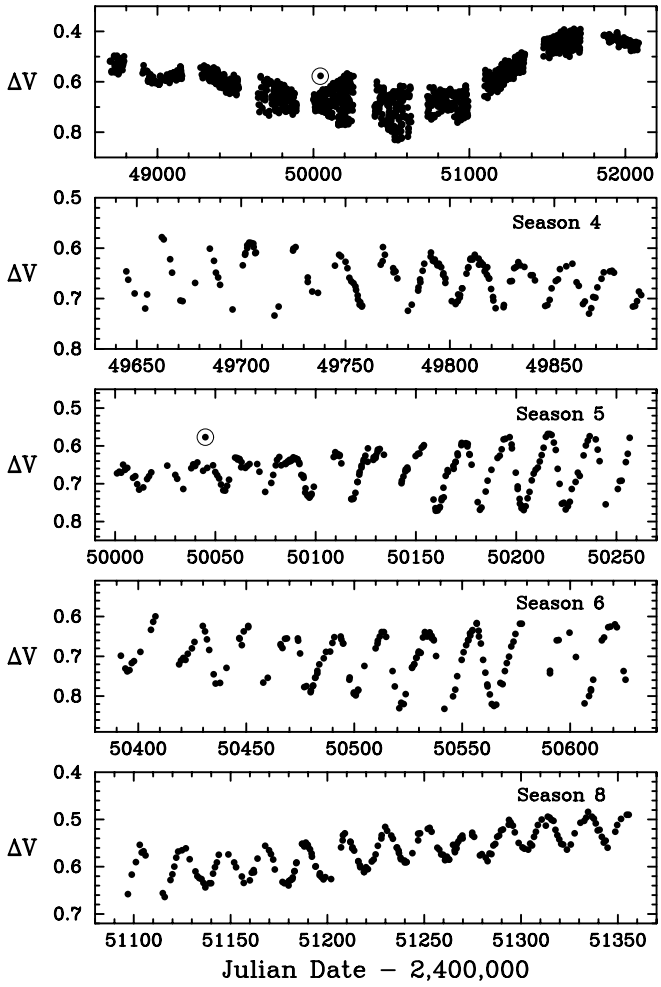

FIG. 2.—Variable minus comparison differential magnitudes of HD 89546 in V from the 0.4 m APT plotted against Julian date. The top panel shows all 10 yr of data, while the remaining panels show selected individual seasons. The circled point in the fifth observing season, shown in both the top and middle panels, is an optical flare observed on HJD 2,450,044.94 = 1995 November 23.44 UT.

TABLE 6
FUNDAMENTAL PROPERTIES OF HD 89546

Parameter	Value	Reference
V (mag)	7.26	This paper
$B-V$ (mag)	0.98	This paper
π (arcsec)	0.00573 ± 0.00083	ESA 1997
Spectral type	G9 III	This paper
$v \sin i$ (km s^{-1})	18.0 ± 1.0	Fekel 1997
M_V (mag)	1.05 ± 0.33	This paper
L ($L_\odot$)	42.1 ± 12.8	This paper
R ($R_\odot$)	9.1 ± 1.4	This paper

the parallax and to a lesser extent in the effective temperature, with the latter uncertainty estimated to be ± 100 K. If the unspotted V magnitude were 0.2 mag brighter than our adopted value, the luminosity would be increased by 20% and the radius by 10%. The various quantities are summarized in Table 6.

By comparing the giant's minimum radius, computed from $v \sin i = 18$ km s^{-1} (Fekel 1997) and a mean rotation period of 21.3 days (§ 4.4), with the radius determined from its *Hipparcos* parallax, a rotational inclination of $57^{\circ}{}^{+22^{\circ}}_{-13^{\circ}}$ was found for the primary. Examining 37 synchronously rotating RS CVn systems, Stawikowski & Glebocki (1994) determined that the rotational and orbital axes are parallel in every case. Thus we assumed that the two axes are also parallel for HD 89546.

Our orbital elements are similar to those of Marino et al. (2002), although, because of our greater number of observing seasons, our orbital period is more accurate. However, we differ somewhat in our derived properties. In particular, from canonical tables of masses, Marino et al. (2002) adopted a mass for the giant of 2.3–2.9 $M_\odot$. Such a large mass is rather unlikely for several reasons. Those masses correspond to a main-sequence spectral class of late-B or early-A and imply that the giant is relatively young. However, its position, about 130 pc above the Galactic plane, and its somewhat metal-poor composition suggest an older, lower mass giant. Thus we initially adopted a primary mass of 1.5 $M_\odot$, typical for evolved chromospherically active stars (Popper 1980). Combining the above inclination value and mass with our mass function of 0.029 $M_\odot$, we found a mass of 0.58 $M_\odot$ for the secondary. Computation of the UVW space motions in a right-handed coordinate system resulted in values of -69, -18, and -6 km s^{-1}, respectively, making HD 89546 a high-velocity star. This suggests that the system may be quite old, with a mass of perhaps 1.0 $M_\odot$ for the primary. Such a value reduces the mass of the secondary to 0.47 $M_\odot$. With a mass range of 1.5–1.0 $M_\odot$ for the primary, if the secondary is a main-sequence star, it is a late-K or M dwarf (Gray 1992).

4.4. *Photometric Analysis*

The $V-C$ differential magnitudes in the V passband from Table 3 are plotted against Julian date in Figure 2. The top panel displays all 10 observing seasons; the remaining panels show selected individual seasons on expanded time axes. We performed separate periodogram analyses for each observing season on both the V and B observations. The resulting periods, which we take to be measures of the stellar rotation period, are given in column (6) of Table 7 along with the Julian date range of each observing season (col. [3]), the number of observations in each season (col. [4]), the seasonal mean $V-C$ differential magnitude (col. [5]), the photometric amplitude (col. [7]), the seasonal mean $K-C$ differential magnitude (col. [8]), and the standard deviation of the $K-C$ differential magnitudes within each season (col. [9]). The weighted mean of the photometric periods for all 10 observing seasons is 21.3 days. The photometric amplitudes were estimated from the light curves; the cited values refer to the cycles with the largest amplitude within each observing season. The largest amplitudes for the whole 10

TABLE 7
RESULTS FROM PHOTOMETRIC ANALYSIS OF HD 89546

Season (1)	Photometric Band (2)	HJD Range (2,400,000+) (3)	N_{obs} (4)	$\langle V-C \rangle$ (mag) (5)	Photometric Period (days) (6)	Peak-to-Peak Amplitude (mag) (7)	$\langle K-C \rangle$ (mag) (8)	σ_{K-C} (mag) (9)
1	V	48,696–48,786	34	0.5347	21.50	0.06	−1.7050	0.0065
1	B	48,696–48,786	32	0.5085	21.59	0.07	−2.3929	0.0083
2	V	48,906–49,156	117	0.5792	21.59	0.05	−1.7040	0.0049
2	B	48,906–49,156	117	0.5605	21.62	0.06	−2.3923	0.0080
3	V	49,276–49,519	158	0.5918	21.60	0.08	−1.7056	0.0052
3	B	49,276–49,520	158	0.5759	21.54	0.09	−2.3876	0.0052
4	V	49,644–49,891	158	0.6575	21.54	0.14	−1.7067	0.0050
4	B	49,644–49,891	161	0.6458	21.54	0.15	−2.3906	0.0054
5	V	50,001–50,256	216	0.6666	21.49	0.20	−1.7086	0.0059
5	B	50,001–50,256	218	0.6568	21.48	0.22	−2.3927	0.0049
6	V	50,392–50,625	159	0.7040	21.22	0.21	−1.7083	0.0048
6	B	50,392–50,625	162	0.6960	21.21	0.24	−2.3897	0.0052
7	V	50,731–50,992	168	0.6766	20.99	0.13	−1.7067	0.0053
7	B	50,731–50,992	167	0.6684	20.98	0.14	−2.3895	0.0055
8	V	51,097–51,355	197	0.5672	20.71	0.09	−1.7059	0.0064
8	B	51,099–51,355	197	0.5499	20.67	0.11	−2.3847	0.0066
9	V	51,474–51,712	139	0.4455	21.21	0.09	−1.7053	0.0061
9	B	51,474–51,712	147	0.4117	21.20	0.12	−2.3857	0.0056
10	V	51,862–52,084	102	0.4414	20.51	0.04	−1.7041	0.0063
10	B	51,862–52,084	101	0.4082	20.24	0.04	−2.3837	0.0058

yr data set (0.21 and 0.24 mag in V and B, respectively) occurred in the sixth season.

The standard deviations of the $K-C$ differential magnitudes in column (9) indicate that both the check and comparison stars are constant from night to night to approximately the limit of our photometric precision with this telescope. The $K-C$ seasonal means, however, vary over a range of 0.004 mag, as shown in Figure 3. While we cannot be sure whether this variation arises from the comparison star or the check star, the amplitude is 100 times smaller than the observed long-term variations in the $V-C$ differential magnitudes and so can have no significant effect on our analysis.

The light curve in the top panel of Figure 2 clearly shows long-term variations in the mean brightness of HD 89546 with a range of $\sim$0.4 mag, suggesting large changes in the average filling factor of spots on the photosphere of the star with a timescale of around 8 yr. If this apparent cycle is analogous to the sunspot cycle in our Sun, we might expect changes in the observed rotation period due to a combination of the star's differential rotation with systematic changes in the spot latitudes as the cycle progresses. We plot the rotation periods versus the observing season in the top panel of Figure 4. The periods plotted are means of the two periods derived separately for each season from the B and V observations. Error bars for each season are estimated from the spread of the B and V periods. Except for season 10, error bars are approximately the size of the plotted points and hence not shown. We see that significant period changes do occur from season to season. However, as seen in panels 2 and 3, these period changes show no correlation with the seasonal mean brightness of HD 89546 or with the amplitude of the light curve, and so they do not appear to be tied to the level of spottedness of the star. We do see a correlation between the amplitude and the mean brightness of HD 89546, as shown in the bottom panel of Figure 4, in the sense that, when the star is fainter and thus has more spots, the rotational modulation of the star's brightness is larger.

The circled observation in the first and third panels of Figure 2 shows HD 89546 to be undergoing an optical flare on HJD 2,450,044.94 = 1995 November 23.44 UT. On that night HD 89546 was anomalously bright by 0.08 and 0.16 mag in V and B, respectively. Good observations the night before and the night after show the star to be at its normal brightness. We have subjected this flare observation in HD 89546 to the same level of scrutiny described in Henry & Hall (1991) for the intense optical flare in V711 Tauri observed with the same APT, and we conclude that this was clearly a real event in HD 89546. Observations of optical flares are quite rare in evolved, chromospherically active stars, including the binary RS CVn stars and the single FK Com stars (Henry & Newsom 1996), in spite of the fact that they are among the most magnetically active of all stars. Only a few of the most active stars in these active groups have been observed to produce intense optical flares (e.g., Henry & Hall 1991 and Foing et al. 1994 in the RS CVn binary V711 Tauri, and Cutispoto, Pagano, & Rodonò 1992 in the FK Com star YY Mensae). The Ca II H and K emission reversals in HD 89546 reach the level of the continuum (Strassmeier 1994) and so certainly place this star among the most active of the RS CVn stars.

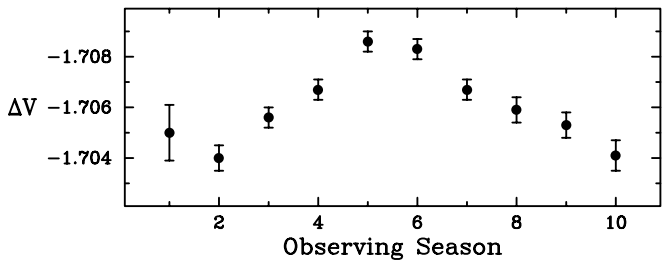

FIG. 3.—Seasonal mean check minus comparison differential magnitudes in V for HD 89546. Slight long-term variability of $\sim$0.004 mag is present in one of the stars but is too small to affect our analysis of the HD 89546 differential magnitudes.

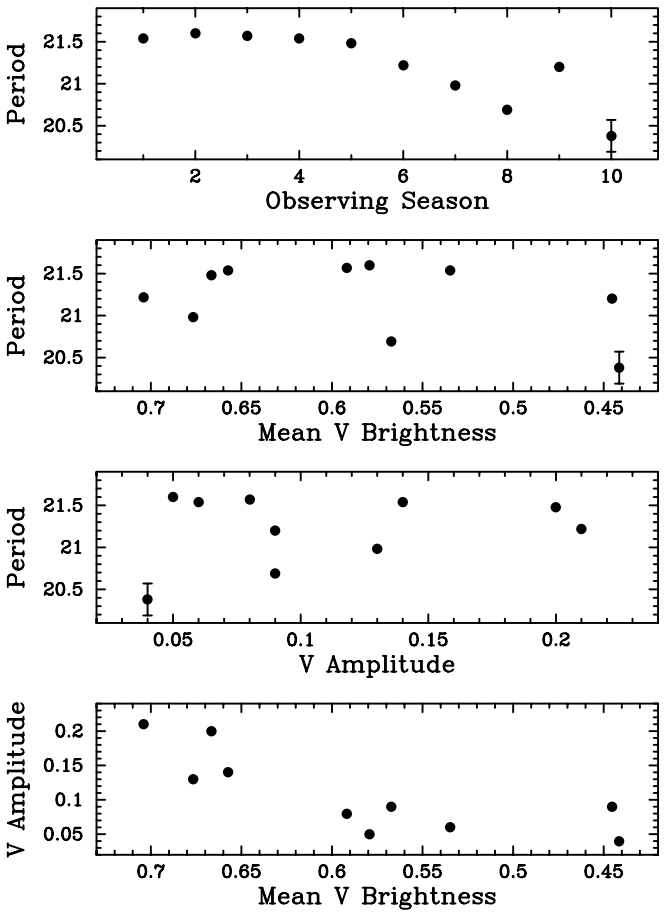

FIG. 4.—Seasonal photometric periods of HD 89546 plotted against time (*top*), against mean brightness of HD 89546 (*second from top*), and V amplitude of the light curve (*third from top*). The V amplitude is plotted against mean brightness (*bottom*).

5. HD 113816 = IS Vir

5.1. *Spectroscopic Orbit*

The spectroscopic orbit of HD 113816 was determined in a manner similar to that for HD 89546 (see § 4.1, where the programs used are more fully described). A preliminary period of 23.66 days was determined from the KPNO velocities in Table 2. This period was adopted to compute initial orbital elements with BISP (Wolfe et al. 1967), which then were refined with SB1 (Barker et al. 1967). Similar orbital solutions were determined for the 31 Coravel velocities. From a comparison of the variances of the two solutions, the Coravel velocities were given weights of 0.15 relative to

TABLE 8
ORBITAL ELEMENTS OF HD 113816

Parameter	Value
P (days)	23.65462 ± 0.00097
T (HJD)	$2{,}449{,}843.4 \pm 1.4$
γ (km s^{-1})	21.252 ± 0.038
K (km s^{-1})	6.598 ± 0.054
e	0.0216 ± 0.0080
ω (deg)	304.5 ± 21.3
$a \sin i$ (km)	$2.146 \pm 0.017 \times 10^6$
$f(m)$ ($M_\odot$)	0.000705 ± 0.000017
Standard error of an observation of unit weight (km s^{-1})	0.23

the KPNO velocities. A simultaneous solution of the two data sets resulted in an orbit with a low eccentricity of 0.0213 ± 0.0074. Thus we computed a circular orbit with SB1C (D. Barlow 1998, private communication). The precepts of Lucy & Sweeney (1971) indicated that the eccentric-orbit solution is to be preferred. The velocities of Buckley et al. (1987) have not been included in the final orbital solution since their addition does not significantly improve the orbital elements. Those velocities are, however, consistent with our solution. We list the orbital elements of our final solution in Table 8. Orbital phases in Table 2 are computed from these elements. The observed velocities and the computed velocity curve are compared in Figure 5, where zero phase is a time of periastron passage.

5.2. *Spectral Type*

The spectral type of HD 113816 was determined by visual comparison with spectra, obtained at KPNO, of early-K subgiant and giant stars from the lists of Keenan & McNeil (1989) and Fekel (1997). The procedure of Strassmeier & Fekel (1990) was employed again. While a couple line ratios suggest a slightly earlier temperature class, the overall appearance of our red-wavelength spectra of HD 113816 is most similar to the spectrum of α Ari, which has a spectral type of K2 III (Keenan & McNeil 1989) and a mean [Fe/H] = −0.22 (Taylor 1999). Since a spectrum synthesis analysis of HD 113816 by Randich et al. (1994) resulted in [Fe/H] = −0.9, we also compared our spectra of HD 113816 with a spectrum of α Boo. This star has a spectral type of K1.5 III (Keenan & McNeil 1989) and a mean [Fe/H] = −0.55 (Taylor 1999). However, in the 6430 Å region, while most of the strong lines are of similar strength in the spectra of both stars, the weak lines of α Boo are not strong enough to match the weak features of HD 113816. Thus we classify HD 113816 as K2 III and suggest that it is only slightly metal-poor compared with the Sun.

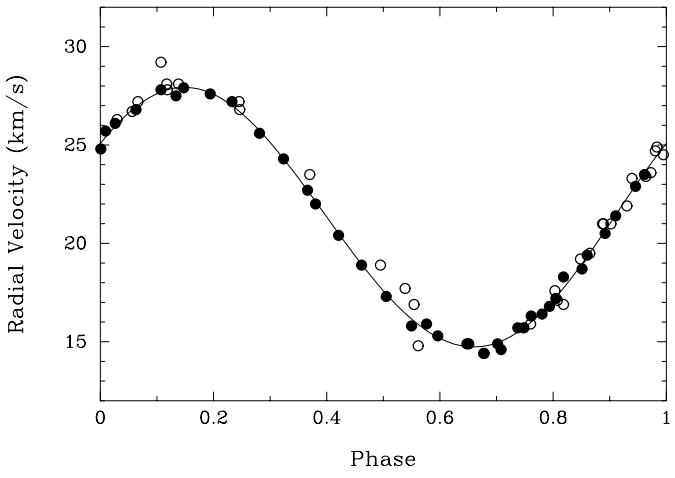

FIG. 5.—Plot of the computed radial-velocity curve of HD 113816 compared with the observations. Filled circles are KPNO velocities; open circles are Coravel velocities. Zero phase is a time of periastron passage.

5.3. *Basic Properties*

We searched the literature and our APT data (below) for the brightest known visual magnitude and corresponding $B-V$ of HD 113816. Buckley et al. (1987) found a V magnitude of 8.27, which is slightly brighter than that for our season 9. Despite the results of O'Neal et al. (1996), we have adopted the historically observed maximum of HD 113816 as the unspotted V magnitude of the primary. This magnitude, combined with the *Hipparcos* parallax (ESA 1997), which corresponds to a distance of 300 ± 84 pc, resulted in $M_v = 0.88 \pm 0.58$ mag. Since HD 113816 is nearly 60° above the Galactic plane, we assumed no interstellar reddening. A $B-V$ color index of 1.15 mag (Buckley et al. 1987) was used in conjunction with Table 3 of Flower (1996) to obtain a bolometric correction and effective temperature. These values were used to compute a luminosity $L = 58.6 \pm 31.2\ L_\odot$ and a radius $R = 12.2 \pm 3.3\ R_\odot$. The uncertainties in the computed quantities are dominated by the uncertainties in the parallax and, to a lesser extent, the effective temperature, with the latter uncertainty estimated to be ±100 K. If the unspotted V magnitude were 0.2 mag brighter than our adopted value, the luminosity would be increased by 20% and the radius by 10%. The various quantities are summarized in Table 9.

Henry et al. (1995) noted that the orbital and photometric periods are essentially equal, indicating that the K giant is

TABLE 9
FUNDAMENTAL PROPERTIES OF HD 113816

Parameter	Value	Reference
V (mag)	8.27	Buckley et al. 1987
$B-V$ (mag)	1.15	Buckley et al. 1987
π (arcsec)	0.00333 ± 0.00087	ESA 1997
Spectral type	K2 III	This paper
$v \sin i$ (km s^{-1})	5.9 ± 1.0	Fekel 1997
M_V (mag)	0.88 ± 0.58	This paper
L ($L_\odot$)	58.6 ± 31.2	This paper
R ($R_\odot$)	12.2 ± 3.3	This paper

synchronously rotating. Its minimum radius is computed from the mean rotation period of 24.1 days (§ 5.4) and the $v \sin i$ value. When compared with the radius determined from its *Hipparcos* parallax, a rotational inclination of $13^\circ \pm 4^\circ$ results, and so the star is seen nearly pole on. From the work of Stawikowski & Glebocki (1994) we assumed that the rotational and orbital axes of HD 113816 are parallel. Thus the equally low orbital inclination partially explains the extremely small mass function of 0.0007 $M_\odot$.

Canonical masses for K giants, such as those of Gray (1992), indicate that the giants evolved from late-B or early-A stars and thus are relatively young. However, HD 113816 is about 250 pc above the Galactic plane, suggesting that the system is substantially older, and so the giant component is unlikely to have such a large mass. Thus, as we did for HD 89546, we have adopted a mass of 1.5 $M_\odot$ from Popper (1980) for the late-type giant of HD 113816. That mass, combined with our mass function and derived inclination of 13°, produces a mass of 0.66 $M_\odot$ for the secondary star, which, if it is a main-sequence object, corresponds to a spectral type of K5 V (Gray 1992).

5.4. *Photometric Analysis*

The $V-K$ differential magnitudes of HD 113816 in the V passband from Table 4 are plotted against Julian date in Figure 6. All 12 observing seasons are shown on the top panel, and selected individual seasons are shown in the remaining panels. The results of our periodogram analyses of the individual seasons are given in Table 10 in the same format as for HD 89546 in Table 7. The weighted mean of the photometric periods is 24.1 days. The amplitudes for each season were estimated from the light curves and never exceeded 0.09 mag.

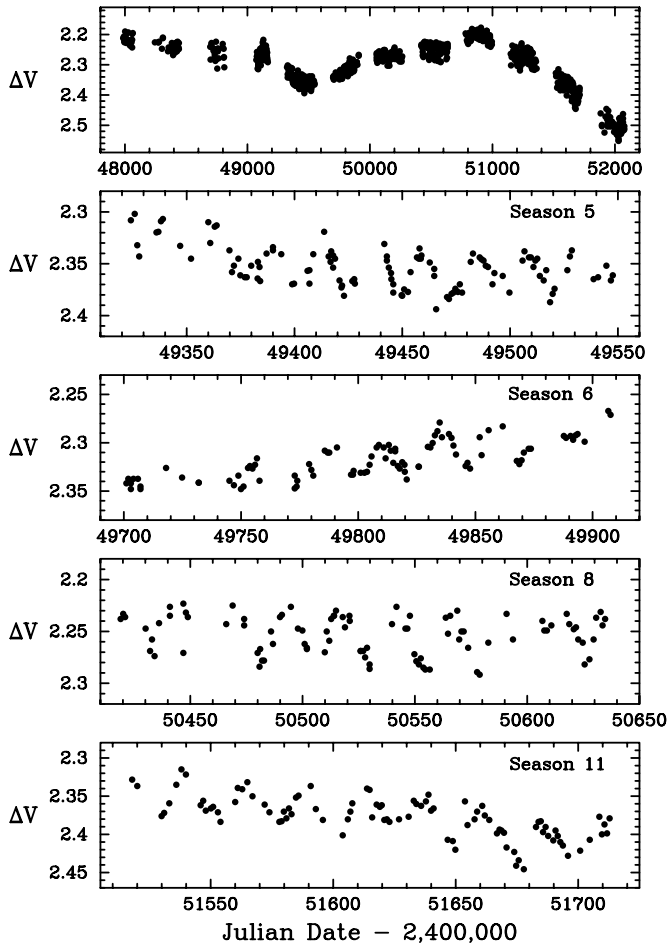

FIG. 6.—Variable minus check differential magnitudes of HD 113816 in V from the 0.4 m APT plotted against Julian date. The top panel shows all 12 yr of data, while the remaining panels show selected individual seasons.

The standard deviations of the $C-K$ differential magnitudes in column (9) indicate that at least one of these two stars is variable. Because a prominent 6.5 day period was found in all the $V-C$ and $K-C$ differential magnitudes, the source of this variability is obviously the comparison star HD 113449, which was shown to be a young, solar-type star in Gaidos, Henry, & Henry (2000) from the analysis of a subset of the observations in Table 4. The seasonal means of the $C-K$ differential magnitudes are plotted in Figure 7 and are seen to vary over a range of $\sim$0.025 mag. Most or all of this long-term variability can also be attributed to the comparison star HD 113449. Thus any remaining variability in the check star HD 111998 must be very small compared with the variability in HD 113816, so we chose to analyze the $V-K$ observations in this case.

The top panel of Figure 6 reveals long-term variations in the mean brightness of HD 113816 similar to HD 89546, with the slightly smaller range of 0.3 mag and a similar timescale of 7–8 yr. Thus it too undergoes large changes in the average filling factor of its photospheric spots. Figure 8 reveals significant period changes in HD 113816. However, as for HD 89546, these changes are not correlated with mean brightness or with photometric amplitude and thus seem unrelated to a possible cycle in the level of spottedness. We also see the same correlation between photometric amplitude and mean brightness as we observed in HD 89546.

As was done above for HD 89546, we searched our HD 113816 data set for optical flares in the manner described in (Henry & Newsom 1996). We found no evidence for any optical flares in HD 113816, even though this star is also among the most active of chromospherically active stars, with Ca II H and K emission reversals that exceed the level of the continuum (Strassmeier 1994).

6. GENERAL DISCUSSION

Standard theory (Iben 1967a, 1967b) predicts that the lithium abundance of a star is significantly diluted as it ascends the red giant branch. This is supported observationally by the survey of Brown et al. (1989), who found that in a sample of nearly 650 giants only about 2% of the stars have LTE abundances $\log \epsilon$ (Li) ≥ 1.5. Over the past decade a small but ever increasing number of post–main-sequence stars (for a recent list see Charbonnel & Balachandran 2000) have been discovered with lithium abundances greater than those predicted from standard theory. In fact, at least two giants, both of which are chromospherically active, have lithium abundances that are greater than the initial value for Population I stars (Balachandran et al. 2000). There are currently two leading explanations for the lithium-rich giants. Following the suggestion of Alexander (1967), Siess & Livio (1999) developed the idea that the unexpectedly high lithium abundances in some giant stars result from the accretion of planets. Alternatively, Charbonnel & Balachandran (2000) recently proposed a scenario in which mixing episodes on the red giant branch and early

TABLE 10
RESULTS FROM PHOTOMETRIC ANALYSIS OF HD 113816

Season (1)	Photometric Band (2)	HJD Range (2,400,000+) (3)	N_{obs} (4)	$\langle V-K \rangle$ (mag) (5)	Photometric Period (days) (6)	Peak-to-Peak Amplitude (mag) (7)	$\langle C-K \rangle$ (mag) (8)	σ_{C-K} (mag) (9)
1.....	*V*	47,987–48,062	27	2.2165	[a]	0.04	1.5846	0.0166
1.....	*B*	47,987–48,062	30	2.8503	[a]	0.04	1.9409	0.0162
2.....	*V*	48,245–48,439	36	2.2396	[a]	0.02	1.5872	0.0125
2.....	*B*	48,245–48,439	40	2.8656	[a]	0.03	1.9389	0.0158
3.....	*V*	48,696–48,809	25	2.2604	[a]	0.02	1.5952	0.0223
3.....	*B*	48,696–48,813	23	2.9169	[a]	0.03	1.9673	0.0222
4.....	*V*	49,071–49,164	56	2.2670	25.62	0.06	1.5937	0.0125
4.....	*B*	49,071–49,164	54	2.9230	25.35	0.06	1.9602	0.0168
5.....	*V*	49,324–49,547	112	2.3530	23.61	0.06	1.5676	0.0093
5.....	*B*	49,324–49,547	113	3.0144	23.56	0.07	1.9261	0.0086
6.....	*V*	49,701–49,907	92	2.3177	24.27	0.05	1.5813	0.0096
6.....	*B*	49,701–49,908	102	2.9713	23.87	0.06	1.9427	0.0110
7.....	*V*	50,053–50,261	118	2.2718	24.24	0.03	1.5728	0.0156
7.....	*B*	50,053–50,261	125	2.9243	24.05	0.02	1.9339	0.0182
8.....	*V*	50,419–50,634	93	2.2532	24.11	0.05	1.5719	0.0149
8.....	*B*	50,419–50,635	102	2.9056	24.02	0.07	1.9302	0.0165
9.....	*V*	50,783–50,994	101	2.2062	23.65	0.04	1.5817	0.0177
9.....	*B*	50,788–50,993	103	2.8530	23.71	0.04	1.9444	0.0201
10.....	*V*	51,149–51,360	99	2.2735	23.49	0.05	1.5763	0.0100
10.....	*B*	51,153–51,360	100	2.9257	23.54	0.06	1.9374	0.0104
11.....	*V*	51,518–51,712	93	2.3770	23.83	0.07	1.5878	0.0114
11.....	*B*	51,518–51,712	89	3.0381	24.00	0.09	1.9519	0.0127
12.....	*V*	51,885–52,075	58	2.5010	24.0[b]	0.08	1.5938	0.0088
12.....	*B*	51,885–52,076	65	3.1761	24.0[b]	0.08	1.9620	0.0095

[a] Data too sparse for period determination.
[b] Period estimated from the light curve.

asymptotic giant branch result in brief periods of enhanced lithium. To date the highest lithium abundances, $\log \epsilon$ (Li) ≥ 2.5, have only been found in chromospherically active *single* giants and not in active binaries.

For HD 89546 Strassmeier et al. (2000) obtained a 6708 Å lithium-line equivalent width of 56 mÅ, which resulted in a log abundance of 1.64. Strassmeier et al. (2000) computed their lithium abundances with the non-LTE curves of growth of Pavlenko & Magazzù (1996). From our spectrum of 1998 October we determined a slightly larger equivalent width of 66 mÅ, which would increase the log abundance by about 0.1. For HD 113816 Randich et al. (1994) determined a log abundance of 0.8, while Strassmeier et al. (2000) found a 6708 Å lithium-line equivalent width of 106 mÅ and obtained a log abundance of 1.7. This large difference is primarily attributable to the non-LTE correction, which increases the LTE log abundance value by 0.3–0.4 (Pavlenko & Magazzù 1996), and also the somewhat higher effective temperature that Strassmeier et al. (2000) used for HD 113816. Thus both chromospherically active giants have lithium abundances in the upper envelope of values for normal giants and are not lithium-rich.

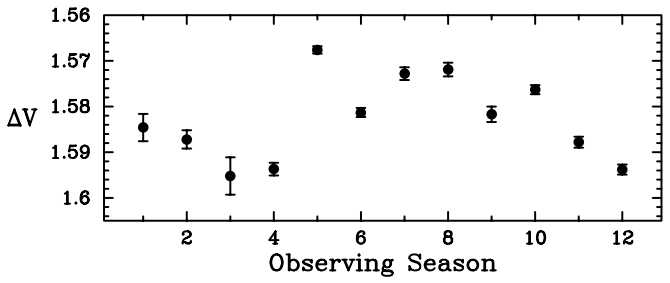

FIG. 7.—Seasonal mean comparison minus check differential magnitudes in *V* for HD 113816. The seasonal means vary over a range of ~0.025 mag, but this variability can be traced to the comparison star HD 113449 and thus will not affect our analysis of the $V-K$ differential magnitudes.

The two main theories of orbital circularization and rotational synchronization (e.g., Zahn, 1977; Tassoul & Tassoul 1992) disagree significantly on absolute timescales but do agree that synchronization should occur first. HD 89546 and HD 113816 have similar orbital periods of 21.4 and 23.7 days, respectively, and both are synchronously rotating. They also have circular or nearly circular orbits, as do the vast majority of chromospherically active binaries with periods less than 30 days (Fekel & Eitter 1989).

Our results indicate that the primary components of HD 89564 and HD 113816 have very similar masses, absolute magnitudes, spectral types, rotation periods, and levels of surface magnetic activity. However, we have shown that we observe them at relatively high and low inclinations, respectively. Therefore, it is of interest to compare the observed starspot activity in these two stars that is documented in Figures 2 and 6. We do so in the context of the random-spot model (RSM) of Eaton, Henry, & Fekel (1996). The RSM uses large numbers (10–40) of moderately sized dark spots placed randomly on a differentially rotating star to reproduce the light curves of chromospherically active stars. The continual redistribution of spots due to stellar differential rotation accounts for much of the changing shape and amplitude of the light curves on rotational timescales. If the spots are also allowed to decay and appear at random on the star with typical lifetimes of several years, then, in addi-

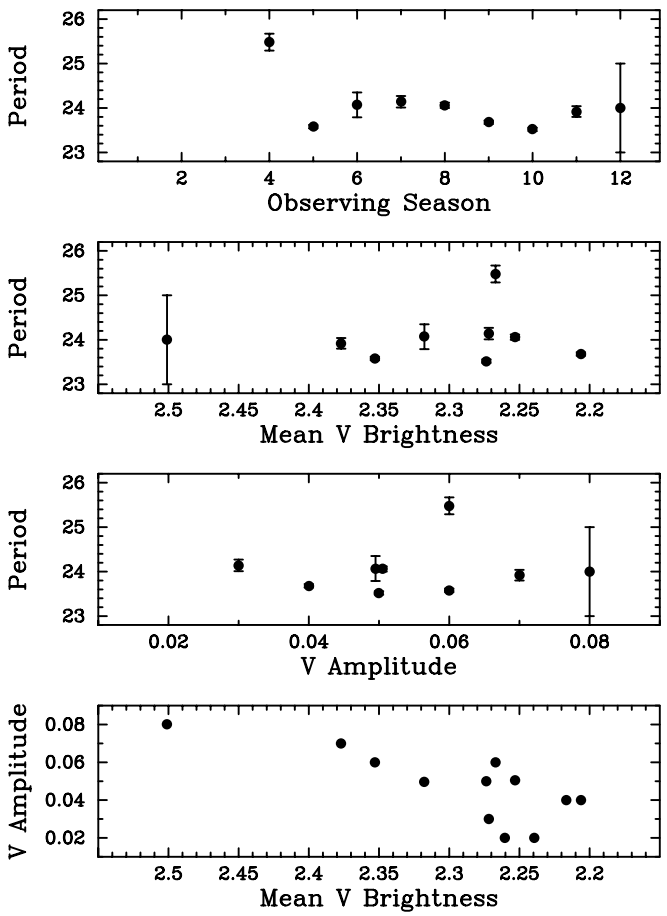

FIG. 8.—Seasonal photometric periods of HD 113816 plotted against time (*top*), against mean brightness of HD 113816 (*second from top*), and V amplitude of the light curve (*third from top*). The V amplitude is plotted against mean brightness (*bottom*).

tion to further changes in the shape of the light curves, the RSM also predicts the kind of long-term light variations observed in most chromospherically active stars without the necessity of magnetic cycles to drive these changes. Eaton, Henry, & Fekel (1996) demonstrated that the RSM does an excellent job of producing light curves that strongly resemble the actual light curves of chromospherically active stars on both rotational and decadal timescales.

There are many similarities in the light curves of HD 89546 and HD 113816. Both show clear rotational modulation within each observing season, as well as changes in the shape and amplitude of the light curve from one rotation cycle to the next (e.g., HD 89546, season 5; HD 113816, end of season 11). These changes can be explained by the continual redistribution of a large number of photospheric spots due to differential rotation. The fifth season of HD 89546 offers a particularly good example of this. The light curve is continually growing in amplitude, while the mean light level remains constant. Since the light level averaged over a rotation cycle must be a measure of the filling factor of spots over the entire visible stellar surface, these changes in amplitude must occur without any change in the overall level of spottedness. Therefore, low amplitudes result when the spots are more uniformly distributed in stellar longitude, while the larger amplitudes result when the same total spot area becomes more concentrated or clumped on one hemisphere by the differential rotation. Indeed when the amplitude is low, and the spots more evenly distributed, a shallow secondary minimum appears in the season 5 light curve, revealing the presence of small spot concentrations on opposite hemispheres. As the amplitude increases, the light-curve shape evolves from this double-humped configuration to an asymmetrical shape with a single maximum and minimum per rotation cycle to a nearly sinusoidal light curve as the spots are continually redistributed.

Both stars sometimes undergo changes in the mean light level during an observing season with little or no corresponding change in rotational amplitude (e.g., HD 89546, season 8; HD 113816, season 6). As long as the amplitudes remain constant, the clumpiness of the spot distributions is not changing. However, in both of these cases the mean brightness is increasing, suggesting that the total spot area is decreasing. With rotational inclinations of 57° and 13°, respectively, both HD 89546 and HD 113816 have significant portions of their photospheres that remain in continual view throughout a rotation cycle and thus do not contribute much to rotational modulation. Thus the decay of a spot or spots in the circumpolar regions would cause an increase in mean brightness with little effect on the amplitude of the light curve. The spots causing the rotational modulation must reside at lower latitudes and remain relatively unchanged during these epochs.

Both stars also experience large, *long-term* changes in mean brightness with timescales of roughly 8 or 9 yr. In fact these long-term brightness changes are larger than any of the rotational amplitudes. The total range in seasonal mean brightness is 0.26 mag in V for HD 89546 (Table 7) and 0.29 mag in V for HD 113816 (Table 10), compared with maximum rotational amplitudes in V of 0.21 mag and 0.08 mag for HD 89546 and HD 113816, respectively. Clearly, both stars experience long-term changes in their overall level of spottedness. As we will show below, these long-term changes can be accounted for in the RSM by the random appearance and decay of individual spots.

Further similarities in these two stars are evident in Figures 4 and 8. Both exhibit period changes on the order of 5% that are not correlated with mean brightness or amplitude. If the rotation periods represent precise determinations of stellar rotation, then we would expect HD 113816 to have a smaller range of periods, since only spots in a very restricted range of stellar latitude can effectively modulate the light curve. However, the observed photometric periods can be affected by the growth and decay of individual spots at various longitudes and also by the formation of new and decay of old clumps of spots by differential rotation. Thus the photometric period at any epoch may not correspond precisely to the rotation period of *any* stellar latitude. It may be that the 5% variation in the observed periods for these two stars is more a function of these effects than a real effect of differential rotation.

Figures 4 and 8 also show that, for each star, the rotational amplitude *is* correlated with the mean brightness level, where larger amplitudes result from greater levels of overall spottedness. This same correlation was found for only one of four well-observed chromospherically active stars in Henry et al. (1995, λ And; their Fig. 23). For σ Gem, II Peg, and V711 Tau, Henry et al. (1995) found no correlation between amplitude and mean brightness (their Figs. 24, 25, and 26). The *lack* of correlation implies that the amplitude changes are due more to spot redistribution than to

any change in overall level of spottedness. In the sample of six stars from Henry et al. (1995) and this paper, half show a definite correlation between amplitude and level of spottedness, and half do not.

The most striking *difference* between the light curves of HD 89546 and HD 113816 is the amplitude of their rotational modulation. As pointed out above, the low inclination of HD 113816 means that only a very restricted range of stellar latitudes can effectively modulate the light curve. Therefore, random distributions of spots with comparable filling factors on these two stars, which is expected from their similar properties and comparable levels of Ca II H and K emission flux (Strassmeier et al. 2000), predict much larger rotational modulation for HD 89546 than for HD 113816. As pointed out above, the maximum rotational amplitude of HD 89546 is nearly 3 times larger than that of HD 113816. The difference in the *ratio* of maximum rotational amplitude to the long-term amplitude (0.81 and 0.28 for HD 89546 and HD 113816, respectively) is also a result of the difference in the rotational inclination of these two stars. For a star viewed pole on, this ratio would necessarily go to zero, since there could be no rotational modulation of the light at all.

Finally, we demonstrate quantitatively that the random-spot model of Eaton, Henry, & Fekel (1996) does reproduce the kinds of light variations discussed above, even for an inclination as low as 13°. We calculated 20 sequences of random-spot models for inclinations of 13°, 30°, and 57°. Each sequence spans 5000 days and starts with different seeds for the random-number generator. All models had 20 spots, a 10 day rotation period, a differential-rotation parameter of $k = 0.01$, and spot lifetimes of 3.0 yr. Figure 9 gives one example for an inclination of 13°; the others are similar. The figure demonstrates that the RSM can produce long-term and short-term variations similar to those seen in Figure 6.

To characterize the light variation, we calculated ΔV, the rms light loss of all 12,500 calculated points from the maximum magnitude in each light curve, and δV, the rms deviation of these points from the means of the individual rotational cycles. For the spot size assumed, all three inclinations gave essentially the amount of long-term light variation seen in plots such as Figure 6, namely, $\langle \Delta V \rangle = 0.17 \pm 0.03$ mag, averaged over all 20 sets of light curves. This result is similar to that found for real chromospherically active stars. The rotational modulation showed a factor of 3 variation over this range of inclination, with $\langle \delta V \rangle = 0.018$, 0.038, and 0.056, respectively, for 13°, 30°, and 57°. This range may be a little larger than would be expected for actual stars. However, even at the very low inclination of 13°, we calculated theoretical light variations at least as big as the maximum observed in HD 113816.

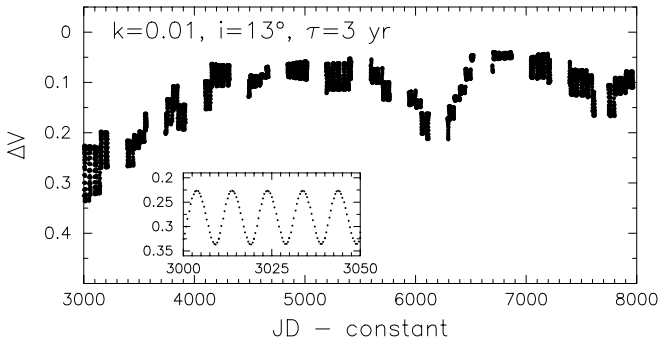

FIG. 9.—Theoretical light curve computed from the random-spot model with a differential-rotation parameter of 0.01 and 20 spots living 3 yr on average. Seen in the figure are long-term light variation and rotational modulation typical of chromospherically active stars. The inset shows the 0.1 mag variation possible with a random distribution of spots even at the low inclination of 13°.

We thank W. Bidelman for communicating his results for HD 89546 in advance of publication. The circular-orbit program provided by D. Barlow is greatly appreciated. We also thank V. Dadonas for his preliminary analysis of some of the velocities and L. Boyd and D. Epand for their efforts in support of Fairborn Observatory. The comments of the referee, G. Cutispoto, resulted in an improved paper. The Automated Astronomy Program at Tennessee State University is supported in part by NASA grants NC-511 and NC-96, and NSF grant HRD 97-06268.

REFERENCES

Alexander, J. B. 1967, Observatory, 87, 238
Balachandran, S. C., Fekel, F. C., Henry, G. W., & Uitenbroek, H. 2000, ApJ, 542, 978
Barden, S. C. 1985, ApJ, 295, 162
Barker, E. S., Evans, D. S., & Laing, J. D. 1967, R. Obs. Bull., 130
Batten, A. H., Fletcher, J. M., & MacCarthy, D. G. 1989, Publ. Dom. Astrophys. Obs., 17, 1
Bidelman, W. P. 1981, AJ, 86, 553
Bidelman, W. P., & MacConnell, D. J. 1973, AJ, 78, 687
Brown, J. A., Sneden, C., Lambert, D. L., & Dutchover, E. 1989, ApJS, 71, 293
Buckley, D. A. H., Tuohy, I. R., Remillard, R. A., Bradt, H. V., & Schwartz, D. A. 1987, ApJ, 315, 273
Charbonnel, C., & Balachandran, S. C. 2000, A&A, 359, 563
Cutispoto, G., Pagano, I., & Rodonò, M. 1992, A&A, 263, L3
Cutispoto, G., Pastori, L., Tagliaferri, G., Messina, S., & Pallavicini, R. 1999, A&AS, 138, 87
Cutispoto, G., Tagliaferri, G., Giommi, P., Gouiffes, C., Pallavicini, R., Pasquini, L., & Rodono, M. 1991, A&AS, 87, 233
Dempsey, R. C., Linnsky, J. L., Fleming, T. A., & Schmitt, J. H. M. M. 1993, ApJS, 86, 599
Eaton, J. A., Henry, G. W., & Fekel, F. C. 1996, ApJ, 462, 888
ESA. 1997, The Hipparcos and Tycho Catalogues (ESA SP-1200) (Noordwijk: ESA)
Fekel, F. C. 1997, PASP, 109, 514
Fekel, F. C., & Eitter, J. J. 1989, AJ, 97, 1139
Fitzpatrick, M. J. 1993, in ASP Conf. Ser. 52, Astronomical Data Analysis Software and Systems II, ed. R. J. Hanisch, R. V. J. Brissenden, & J. Barnes (San Francisco: ASP), 472
Fleming, T. A., Gioia, I. M., & Maccacaro, T. 1989, AJ, 98, 692
Flower, P. J. 1996, ApJ, 469, 355
Foing, B. H., et al. 1994, A&A, 292, 543
Gaidos, E. J., Henry, G. W., & Henry, S. M. 2000, AJ, 120, 1006
Gray, D. F. 1992, The Observation and Analysis of Stellar Photospheres (Cambridge: Cambridge University Press)
Henry, G. W. 1995a, in ASP Conf. Ser. 79, Robotic Telescopes: Current Capabilities, Present Developments, and Future Prospects for Automated Astronomy, ed. G. W. Henry & J. A. Eaton (San Francisco: ASP), 37
———. 1995b, in ASP Conf. Ser. 79, Robotic Telescopes: Current Capabilities, Present Developments, and Future Prospects for Automated Astronomy, ed. G. W. Henry & J. A. Eaton (San Francisco: ASP), 44
Henry, G. W., Eaton, J. A., Hamer, J., & Hall, D. S. 1995, ApJS, 97, 513
Henry, G. W., Fekel, F. C., & Hall, D. S. 1995, AJ, 110, 2926
Henry, G. W., & Hall, D. S. 1991, ApJ, 373, L9
Henry, G. W., & Newsom, M. S. 1996, PASP, 108, 242
Henry, T. J., Soderblom, D. R., Donahue, R. A., & Baliunas, S. L. 1996, AJ, 111, 439
Huenemoerder, D. P., & Barden, S. C. 1984, BAAS, 16, 510
Iben, I. 1967a, ApJ, 147, 624
———. 1967b, ApJ, 147, 650
Jeffries, R. D., Bertram, D., & Spurgeon, B. R. 1995, MNRAS, 276, 397

Kazarovets, E. V., & Samus, N. N. 1997, Inf. Bull. Variable Stars, 4471, 1
Keenan, P. C., & McNeil, R. C. 1989, ApJS, 71, 245
Lucy, L. B., & Sweeney, M. A. 1971, AJ, 76, 544
Marino, G., Catalano, S., Frasca, A., Marilli, E., & Teriaca, L. 2002, Inf. Bull. Variable Stars, 5227, 1
Montes, D., Fernández-Figueroa, M. J., De Castro, E., Cornide, M., Latorre, A., & Sanz-Forcada, J. 2000, A&AS, 146, 103
Neuhaüser, R., Torres, G., Sterzik, M. F., & Randich, S. 1997, A&A, 325, 647
O'Neal, D., Saar, S., & Neff, J. E. 1996, ApJ, 463, 766
Pavlenko, Y. V., & Magazzù, A. 1996, A&A, 311, 961
Popper, D. M. 1980, ARA&A, 18, 115
Randich, S., Giampapa, M. S., & Pallavicini, R. 1994, A&A, 283, 893
Scarfe, C. D., Batten, A. H., & Fletcher, J. M. 1990, Publ. Dominion Astrophys. Obs., 18, 21
Schwope, A. D., et al. 2000, Astron. Nachr., 321, 1
Siess, L., & Livio, M. 1999, MNRAS, 308, 1133
Stawikowski, A., & Glebocki, R. 1994, Acta Astron., 44, 393
Strassmeier, K. G. 1994, A&AS, 103, 413
Strassmeier, K. G., Bartus, J., Cutispoto, G., & Rodono, M. 1997, A&AS, 125, 11
Strassmeier, K. G., & Fekel, F. C. 1990, A&A, 230, 389
Strassmeier, K. G., Handler, G., Paunzen, E., & Rauth, M. 1994, A&A, 281, 855
Strassmeier, K. G., Washuettl, A., Granzer, Th., Scheck, M., & Weber, M. 2000, A&AS, 142, 275
Tagliaferri, G., Cutispoto, G., Pallivicini, R., Randich, S., & Pasquini, L. 1994, A&A, 285, 272
Tassoul, J.-L., & Tassoul, M. 1992, ApJ, 395, 259
Taylor, B. J. 1999, A&AS, 134, 523
Tokovinin, A. 1987, AZh, 64, 196
Upgren, A. R., & Staron, R. T. 1970, ApJS, 19, 367
Upgren, A., Sperauskas, J., & Boyle, R. P. 2002, Baltic Astron., 11, 91
Wolfe, R. H., Horak, H. G., & Storer, N. W. 1967, in Modern Astrophysics, ed. M. Hack (New York: Gordon & Breach), 251
Zahn, J.-P. 1977, A&A, 57, 383